

# The non-symmetric ion-atom radiative processes in the stellar atmospheres

A. A. Mihajlov<sup>1,3\*</sup>, Lj. M. Ignjatović<sup>1,3</sup>, V. A. Srećković<sup>1,3</sup>,  
M. S. Dimitrijević<sup>2,3</sup> and A. Metropoulos<sup>4</sup>

<sup>1</sup>University of Belgrade, Institute of Physics, P. O. Box 57, 11001 Belgrade, Serbia

<sup>2</sup>Astronomical Observatory, Volgina 7, 11160 Belgrade 74, Serbia

<sup>3</sup>Isaac Newton Institute of Chile, Yugoslavia Branch

<sup>4</sup>Theoretical and Physical Chemistry Institute, NHRF, Athens, Greece

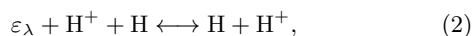
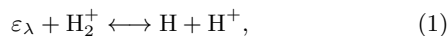
## ABSTRACT

The aim of this research is to show that the processes of absorption charge-exchange and photo-association in  $A + B^+$  collisions together with the processes of  $AB^+$  photo-dissociation in the case of strongly non-symmetric ion-atom systems, significantly influence the opacity of stellar atmospheres in ultraviolet (UV) and extreme UV (EUV) region. In this work, the significance of such processes for solar atmosphere is studied. In the case of the solar atmosphere the absorption processes with  $A = \text{H}$  and  $B = \text{Mg}$  and  $\text{Si}$  are treated as dominant ones, but the cases  $A = \text{H}$  and  $B = \text{Al}$  and  $A = \text{He}$  and  $B = \text{H}$  are also taken into consideration. The choice of just these species is caused by the fact that, of the species relevant for the used solar-atmosphere model, it was only for them that we could determine the necessary characteristics of the corresponding molecular ions, i.e. the molecular potential curves and dipole matrix elements. It is shown that the efficiency of the examined non-symmetric processes within the rather wide corresponding quasi-molecular absorption bands in the far-UV and EUV regions is comparable and sometimes even greater than the intensity of the known symmetric ion-atom absorption processes, which are included now in the models of the solar atmosphere. Consequently, the presented results suggest that the non-symmetric ion-atom absorption processes also have to be included *ab initio* in the corresponding models of the stellar atmospheres.

**Key words:** atomic processes – molecular processes – radiation mechanisms: general – radiative transfer – stars: atmospheres

## 1 INTRODUCTION

Significant influence of at least some of the ion-atom radiative processes on the optical characteristics of the solar atmosphere has already been established. Here we mean the following symmetric processes of molecular ion photo-dissociation/association and radiative charge exchange in ion-atom collisions



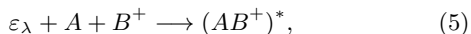
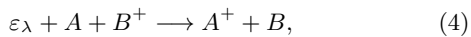
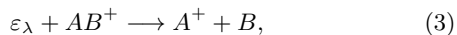
which were studied in the context of the atmosphere of the Sun in (Mihajlov & Dimitrijević 1986; Mihajlov et al. 1993, 1994b, 2007). Let us note that here  $\text{H} = \text{H}(1s)$ ,  $\text{H}_2^+$  is the

molecular ion in the ground electronic state, and  $\varepsilon_\lambda$  - the energy of a photon with wavelength  $\lambda$ . Of course, the results obtained in the mentioned articles are significant and for atmospheres of other solar or near solar type stars.

Only the processes (1) and (2) were taken into account in the mentioned papers, since the contribution of other symmetric ion-atom radiative processes to the solar-atmosphere opacity could be completely neglected due to the composition of the atmosphere, while the possible non-symmetric processes were excluded from the consideration because of the orientation of the research, already established in the first paper (Mihajlov & Dimitrijević 1986), towards the visible and near UV and IR parts of the electro-magnetic (EM) spectrum. However, in Mihajlov et al. (2007) it was demonstrated that the efficiency of the processes (1) and (2) becomes close to the total efficiency of the concurrent electron-ion and electron-atom radiative processes outside of these

\* E-mail: mihajlov@ipb.ac.rs

parts of the EM spectrum, namely in far UV and EUV regions. It is important that just these spectral regions are very significant in the case of the solar atmosphere. This is caused by the fact that the solar emission in far UV and EUV regions very strongly affects the ionosphere every day, and by extension the whole of the Earth's atmosphere. Therefore the solar EM emission in the mentioned regions has been the object of extensive investigation for a long time (see the classic book: White (1977)), which continues up until now (see e.g. Worden et al. (2001); Woods (2008); Woods et al. (2009)). It is clear that in this context it becomes necessary to pay attention not only to the symmetrical ion-atom processes (1) and (2), but also to each new process which might affect the mechanisms of EM radiation transfer in far UV and EUV regions in the solar atmosphere, and consequently the corresponding optical characteristics. These facts suggested that it could be useful to carefully examine also the possible influence of the relevant non-symmetric ion-atom radiative processes on the solar-atmosphere opacity, namely



where  $B$  is an atom in the ground state with its ionization potential  $I_B$  smaller than the ionization potential  $I_A$  of the atom  $A$ , while  $AB^+$  and  $(AB^+)^*$  are the corresponding molecular ions in the electronic states which are asymptotically correlated with the states of the systems  $A + B^+$  and  $A^+ + B$  respectively, and the possible partners are determined by the used solar-atmosphere models. One can see that the processes (3) and (4) represent the analogues of the processes (1) and (2), while the process (5) does not have a symmetric analogue. In this work the standard non-LTE model C for the solar atmosphere from Vernazza et al. (1981) is used. The reason is the fact that as yet all the relevant data needed for our calculations are provided in the tabular form only for this model, and that in Stix (2002) the solar atmosphere model C from Vernazza et al. (1981) is treated as an adequate non-LTE model. In accordance to the chosen model here we take into account the non-symmetric processes (3-5) with  $A = \text{H}(1s)$  and  $B = \text{Mg}, \text{Si}, \text{Fe}$  and  $\text{Al}$ , as well as with  $A = \text{He}(1s^2)$  and  $B = \text{H}(1s)$ . For the solar photosphere the behavior of the densities of the metal  $\text{Mg}^+, \text{Si}^+, \text{Fe}^+$  and  $\text{Al}^+$  ions is particularly important. Namely, in accordance with the Tab's 12, 17 and 19-22 from Vernazza et al. (1981) this behavior, as well as the behavior of the temperature  $T$  and the ion  $\text{H}^+$  density, within the solar photosphere can be illustrated by the Fig.1, where  $h$  is the height of the considered layer with the respect to the chosen referent one. The region of  $h$  is chosen here in accordance with the Fig.4 from the previous paper Mihajlov et al. (2007), where the relative efficiencies of the symmetric ion-atom processes (1) and (2) with the respect to the relevant concurrent (electron-atom and electron-ion) radiative processes are presented. This region is slitted in three parts: two denoted with I, which corresponds to the areas where the efficiency of the processes (1) and (2) with  $A = \text{H}$  is close to the one of the mentioned concurrent processes, and one denoted with II, where their efficiencies can be neglected. From the figure 1 one can see that in the parts

I the ion  $\text{H}^+$  density dominates with the respect to all metal ion  $B^+$  densities, which means that within these parts it is expected that the efficiency of the symmetric processes (1) and (2) is more greater than the one of the non-symmetric processes (3-5). However, from the same figure one can see also that:

- in the part II, i.e. in the neighborhood of the temperature minimum, each of the ion  $B^+$  densities is greater then the ion  $\text{H}^+$  density,

- the width of the part II is close to the total width of the parts denoted with I.

From here it follows that, in the principle, the contribution of the non-symmetric processes (3-5) to the solar atmosphere opacity can be comparable to the one of the symmetric processes (1) and (2), since in the both non-symmetric and symmetric cases as the neutral partner the same atom  $\text{H}$  appears, and that symmetric and non-symmetric ion-atom radiative processes together could be treated as a serious partner to the above mentioned concurrent processes in the whole solar photosphere.

In the general case of the partially ionized gaseous plasmas, apart of the absorption processes (3-5), it is necessary to consider also the corresponding inverse emission processes, namely: the emission charge exchange and photo-association in  $A^+ + B$  collisions, and the photo-dissociation of the molecular ion  $(AB^+)^*$ . However, here only the absorption processes (3) and (4) have to be taken into account. Namely, under the conditions from Vernazza et al. (1981) the influence of the emission processes in  $A^+ + B$  collisions on the optical characteristics of the considered atmospheres can be neglected in comparison to the other relevant emission processes, since both  $A^+$  and  $B$  partners belong to the poorly represented components.

From the beginning of our investigations of ion-atom radiative processes as the final aim we have always the inclusion of the considered processes in the stellar atmospheres models. Here it should be noted that we considered as our task only to provide the relevant data (the corresponding spectral absorption coefficients etc.), which are needed for the stellar atmospheres modeling, without involving into the process of the modeling itself. Consequently, for us it was important only to know whether the processes, which we studied in connection with the considered stellar atmosphere, are included in the corresponding models or not. So during the previous investigations, whose results were published in Mihajlov & Dimitrijević (1986); Mihajlov et al. (1993, 1994b, 2007), we reliably knew that, for example, the processes of the radiative charge-exchange 2 generally were not taken into account in connection with the solar atmosphere. Apart of that, it was known that the photo-dissociation processes 1 were seriously treated only when the atom and ion ( $\text{H}$  and  $\text{H}^+$ ) densities are close, while our results suggested that the processes (1) and (2) are of the greatest importance for the weakly ionized stellar layers (ion density/atom density  $\lesssim 10^{-3}$ ). These reasons fully justified the mentioned investigations. It is important that the situation about the symmetric processes (1) and (2) begins to change now in the positive way, since these processes are already included in some solar atmosphere models (Fontenla et al. 2009).

The main aim of this work is to draw attention to the non-symmetric radiative processes (3)-(5) as the factors of

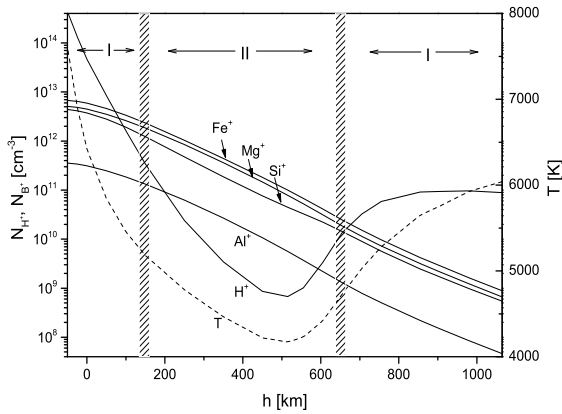


**Figure 1.** The behavior of the temperature  $T$  and the densities  $N_{H^+}$  and  $N_{B^+}$  of the ions  $H^+$  and the metal ions  $B^+$  for the non-LTE model C from Vernazza et al. (1981) within the solar atmosphere.

the influence on the solar atmosphere opacity in the significant parts of UV and EUV regions and, in accordance with above mentioned, to show that these processes should be included *ab initio* in the solar atmosphere models, as well as in the models of solar and near solar type stars, together with the symmetric processes (1) and (2). In this context we will have to determine here the corresponding spectral absorption coefficients, as the functions of  $\lambda$ , the local temperature  $T$  and the relevant particle densities, for the conditions which correspond to the photosphere of the Sun. For that purpose the needed characteristics of the considered ion-atom systems, i.e. the molecular potential curves and dipole matrix elements, are presented in Section 2. Then, the relevant characteristics of these processes themselves, i.e. the mean thermal cross-sections for the photo-dissociation processes (3), and the spectral rate coefficients for the absorption charge exchange processes (4) and (5), will be presented in Section 3. With the help of these characteristics in Section 4 will be calculated the total spectral absorption coefficients, characterizing (3), (4) and (5) absorption processes as the functions of  $\lambda$  and the position within the solar photosphere. Finally, the values of the parameters which characterize the relative contribution of the non-symmetric processes (3)-(5) with the respect to the total contribution of the symmetric and non-symmetric radiative processes (1)-(5), which are also calculated in Section 4, presents the one of the main results of this work. Because of the properties of the considered strongly non-symmetric ion-atom systems only the far-UV and EUV regions of  $\lambda$  are treated here. Let us note that we were able to determine the relevant characteristics of the molecular ions  $HB^+$  for the cases  $B = \text{Mg}, \text{Si}$  and  $\text{Al}$ , and consequently only these cases are considered within this work.

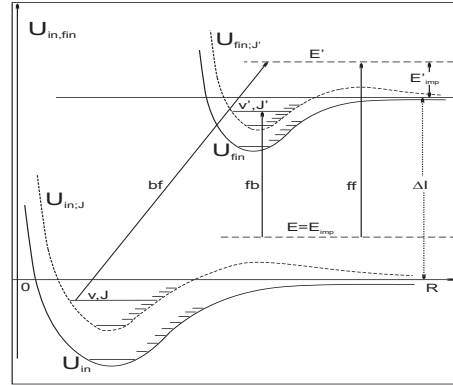


**Figure 2.** Schematic presentation of the non-symmetric processes (3-5) caused by the bf-, ff-, and fb-radiative transitions:  $\Delta I = I_A - I_B$ , where  $I_A$  and  $I_B$  are ionization potentials of the atoms  $A$  and  $B$ ;  $E = E_{imp}$  and  $E'_{impa}$  - the impact energies of the corresponding ion-atom systems;  $U_{in;J}(R)$  and  $U_{fin;J'}(R)$  - are the effective potentials, given by equation (12).

## 2 THE PROPERTIES OF THE NON-SYMMETRIC ION-ATOM SYSTEMS

As in the previous papers the ion-atom radiative processes are described here within two basic approximations: the adiabatic approximation for the relative motion of the nucleus of the considered ion-atom systems, and the dipole approximation for the interaction of these systems with the free electromagnetic field. Since these approximations are discussed in details in the literature (see for example Mihajlov & Popović (1981)), the corresponding matter is considered here briefly, with references only to the elements specific just for the non-symmetric processes (3-5), which are schematically shown in Fig. 2.

In accordance with Fig. 2 the photo-dissociation (bound-free) processes (3), charge-exchange absorption (free-free) processes (4), and photo-association (free-bound) processes (5) are caused by the radiative transitions

$$\begin{aligned} |in; R \rangle &\rightarrow |in, J, v; R \rangle \rightarrow |fin; R \rangle |fin, J', E'; R \rangle, \\ |in; R \rangle &\rightarrow |in, J, E; R \rangle \rightarrow |fin; R \rangle |fin, J', E'; R \rangle, \\ |in; R \rangle &\rightarrow |in, J, E; R \rangle \rightarrow |fin; R \rangle |fin, J', v'; R \rangle, \end{aligned} \quad (6)$$

where  $|in; R \rangle$  and  $|in, J, v; R \rangle$  are initial, and  $|fin; R \rangle$  and  $|fin, J', E'; R \rangle$ ,  $|fin; R \rangle$  and  $|fin, J', v'; R \rangle$  are final states of considered ion-atom system, determined as the products of the adiabatic electronic states  $|in; R \rangle$  and  $|fin; R \rangle$  and the corresponding states which describe relative nucleus motion, and  $R$  denotes the internuclear distance. It is assumed that these transitions are allowed by the dipole selective rules.

From Fig.2 one can see that:

- $|in; R \rangle$  and  $|fin; R \rangle$  belongs to the groups (i) and (ii) of the states of the molecular ions  $AB^+$  and  $(AB^+)^*$  which are asymptotically correlated with the electronic states of the ion-atom systems  $A + B^+$  and  $A^+ + B$  respectively;
- $|in, J, v; R \rangle$  and  $|fin, J', v'; R \rangle$  are the bound rovibrational states of the same molecular ion, defined by the orbital quantum numbers  $J$  and  $J'$  and vibrational quantum numbers  $v$  and  $v'$ ;
- $|in, J, E; R \rangle$  and  $|fin, J', E'; R \rangle$  are the free states of the

same molecular ion defined by the orbital quantum numbers  $J$  and  $J'$  and the total energies  $E$  and  $E'$ . Let us note that as zero of energy here is taken the total energy of the immobile atom  $A$  and ion  $B^+$  at  $R = \infty$ .

The states  $|in, J, v; R\rangle$ ,  $|in, J, E; R\rangle$ ,  $|fin, J', E'; R\rangle$  and  $|fin, J', v'; R\rangle$  are determined as the solutions of the corresponding Schrodinger equations

$$\left[-\frac{1}{2\mu}\Delta + U_{in;J}(R)\right]|in, J, v; R\rangle = \epsilon_{J,v} \cdot |in, J, v; R\rangle, \quad (7)$$

$$\left[-\frac{1}{2\mu}\Delta + U_{in;J}(R)\right]|in, J, E; R\rangle = E \cdot |in, J, E; R\rangle, \quad (8)$$

$$\left[-\frac{1}{2\mu}\Delta + U_{fin;J'}(R)\right]|fin, J', E'; R\rangle = E'_{imp} \cdot |fin, J', E'; R\rangle, \quad (9)$$

$$\left[-\frac{1}{2\mu}\Delta + U_{fin;J'}(R)\right]|fin, J', E'; R\rangle = \epsilon'_{J',v'} \cdot |fin, J', E'; R\rangle, \quad (10)$$

where  $\mu$  is the reduced mass of the considered ion-atom system,

$$E'_{imp} = E' - (I_A - I_B), \quad (11)$$

and  $\epsilon'_{J',v'} < 0$ . With  $U_{in;J}(R)$  and  $U_{fin;J'}(R)$  are defined the effective potential energies given by

$$U_{in;J}(R) = U_{in}(R) + \frac{\hbar^2 J(J+1)}{2\mu R^2}, \quad (12)$$

$$U_{fin;J'}(R) = U_{fin}(R) + \frac{\hbar^2 J'(J'+1)}{2\mu R^2},$$

where  $U_{in}(R)$  and  $U_{fin}(R)$  are the adiabatic potential energies of the molecular ions  $AB^+$  and  $(AB^+)^*$  in the states  $|in; R\rangle$  and  $|fin; R\rangle$  as the functions of  $R$ . In further consideration it is assumed that the radial wave functions which correspond to the considered states satisfy the standard ortho-normalization conditions.

In the case  $A = \text{He}$  and  $B = \text{H}$ , as well as in the cases  $A = \text{H}$  and  $B = \text{Mg}$  or  $\text{Al}$ , each of the groups (i) and (ii) of the electronic molecular states contains only one  $\Sigma$ -state: the ground and the first excited electronic state of the considered molecular ion. Because of that in these cases we will denote the states  $|in; R\rangle$  and  $|fin; R\rangle$  with  $|1; R\rangle$  and  $|2; R\rangle$  respectively, and the corresponding potential curves - with  $U_1(R)$  and  $U_2(R)$ . Let  $D_{in;fin}(R)$  be the electronic dipole matrix element which corresponds to the transitions given in Eqs. (6), i.e.

$$D_{in;fin}(R) = \langle in; R | \mathbf{D}(R) | fin; R \rangle, \quad (13)$$

where  $\mathbf{D}$  is the operator of the dipole moment of the considered ion-atom system. One can see that in the mentioned cases

$$D_{in;fin}(R) = D_{1;2}(R) \equiv \langle 1; R | \mathbf{D}(R) | 2; R \rangle. \quad (14)$$

However, in the case  $A = \text{H}$  and  $B = \text{Si}$ , the group (i) contains the ground electronic  $\Sigma$ -state and the excited, weakly bounded  $\Pi$ -state, denoted here with  $|1a; R\rangle$  and  $|1b; R\rangle$  respectively, while the group (ii) contains two  $\Sigma$ -states and one  $\Pi$ -state, denoted here with  $|2a; R\rangle$ ,  $|2b; R\rangle$  and  $|2c; R\rangle$  respectively. In accordance with this, the corresponding potential curves will be denoted by  $U_{1a,1b}(R)$  and  $U_{2a,2b,2c}(R)$ . One can see that, in this case we have the situations when  $|in, R\rangle = |1a; R\rangle$  and  $|fin, R\rangle = |2a; R\rangle$  or

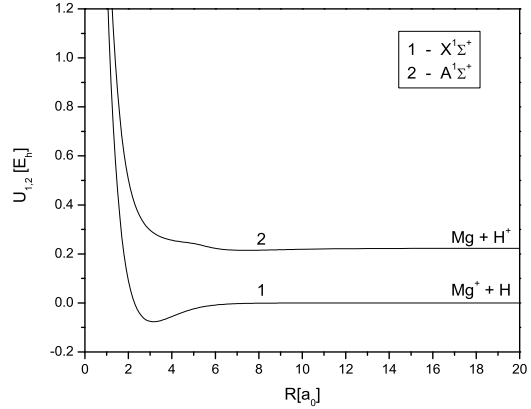


**Figure 3.** The potential curves of the molecular ion  $\text{HMg}^+$ .

$|2b; R\rangle$ , and  $|in, R\rangle = |1b; R\rangle$  and  $|fin, R\rangle = |2c; R\rangle$ . Consequently, the corresponding  $D_{in;fin}(R)$  will be defined here by the relations

$$D_{in;fin}(R) = \begin{cases} D_{1a;2a}(R) \equiv \langle 1a; R | \mathbf{D}(R) | 2a; R \rangle \\ D_{1a;2b}(R) \equiv \langle 1a; R | \mathbf{D}(R) | 2b; R \rangle \\ D_{1b;2c}(R) \equiv \langle 1b; R | \mathbf{D}(R) | 2c; R \rangle \end{cases} \quad (15)$$

For the ions  $\text{HeH}^+$  and  $(\text{HeH}^+)^*$  the potential curves  $U_{1,2}(R)$  and the values of  $D_{1;2}(R)$  are taken from Green et al. (1974b,a). For all other considered molecular ions the corresponding potential curves and the values of the dipole matrix elements are calculated within this work. Also, we will introduce the so called splitting term  $U_{in;fin}(R)$ , defined by

$$U_{in;fin}(R) = U_{fin}(R) - U_{in}(R), \quad (16)$$

which is used in the further considerations.

All calculations were done at the multi-configuration self-consistent field (MCSCF) and multi-reference configuration interaction (MRCI) levels (with MCSCF orbitals) using the MOLPRO package of programs (MOLPRO 2006). The basis sets we employed were the cc-pvqz basis sets of Dunning et al. (Dunning 1989; Kendall et al. 1992). Initially, test runs were done in the asymptotic region (30 Bohr) at the lowest three to five levels at each selected symmetry to determine the low lying levels corresponding to the  $\text{H}-B^+$  and the  $\text{H}^+-B$  electron distributions and their wave functions ( $B = \text{Mg}, \text{Si}, \text{Al}$ ). For each level a Mulliken population analysis was done to determine the location of the charges. Since H has the highest ionization potential, the lowest states of a given symmetry correspond to the  $\text{H}-B^+$  charge distribution while the  $\text{H}^+-B$  charge distribution is described by one or more of the excited states. The potential energies of all these states were calculated starting at the asymptotic region and moving inwards. At each point the dipole matrix elements between the  $\text{H}-B^+$  and  $\text{H}^+-B$  states were calculated using the corresponding wave functions. The calculated potential curves are presented in Figs. 3-5. Figures 6-8 show the behavior of  $D_{1;2}(R)$ ,  $D_{1a;2a;b}(R)$  and  $D_{1b;2c}(R)$ .

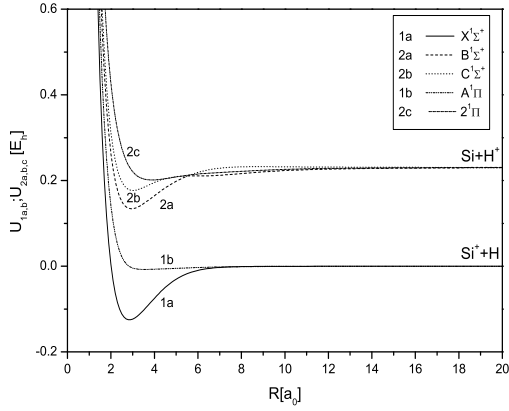


Figure 4. Same as in Fig.3, but for the molecular ion  $\text{HSi}^+$ .

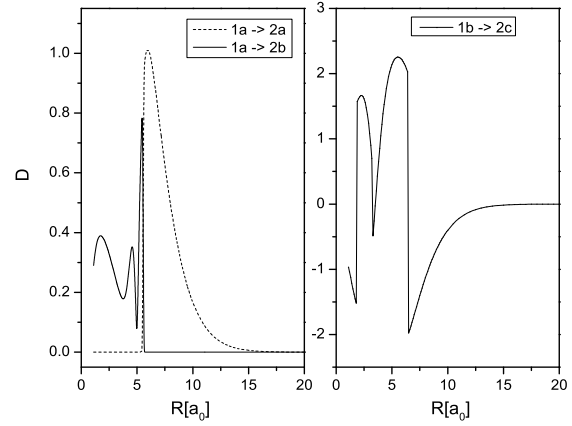


Figure 7. The behavior of dipole matrix elements  $D_{1a;2a;b}(R)$  and  $D_{1b;2c}(R)$ , given by equations (13) and (15), for the molecular ion  $\text{HSi}^+$ .

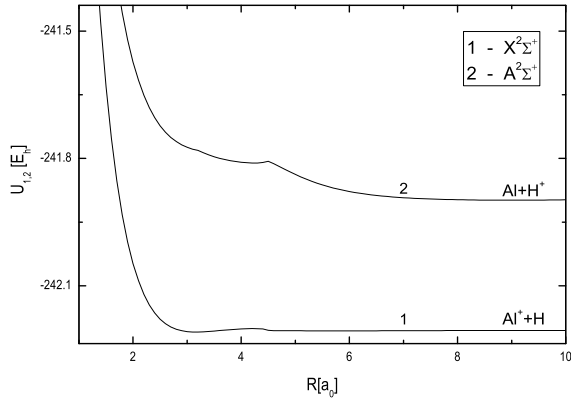


Figure 5. Same as in Fig.3, but for the molecular ion  $\text{HA1}^+$ .

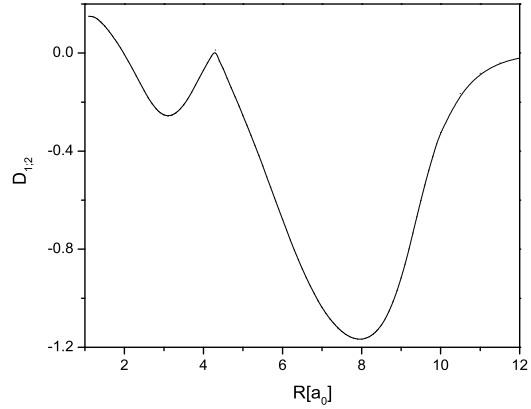


Figure 8. Same as in Fig.6, but for the molecular ion  $\text{HA1}^+$ .

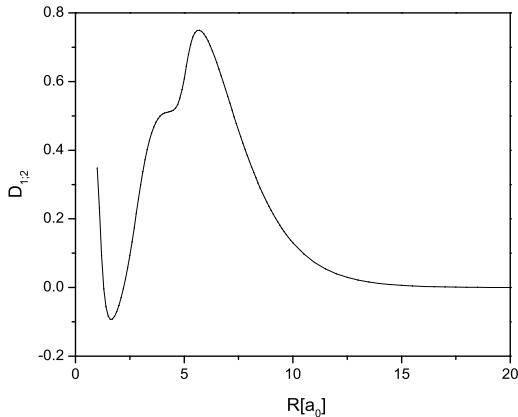


Figure 6. The behaviour of the electronic dipole matrix element  $D_{1,2}(R)$ , given by equations (13) and (14), for the molecular ion  $\text{HMg}^+$ .

### 3 THE RELEVANT SPECTRAL CHARACTERISTICS

In accordance with the aim of this work the considered absorption processes will be characterized by the adequately defined spectral absorption coefficients. We will start from the bound-free, free-free and free-bound absorption processes, caused by the radiative transitions given by Eqs.(6), for the given species  $A$  and  $B$ . In the cases  $A = \text{H}$  and  $B = \text{Mg}$  and  $A = \text{He}$  and  $B = \text{H}$  where the transitions given by Eqs.(6) are connected with only one initial and one final  $\Sigma$ -electronic state, the corresponding spectral absorption coefficients are denoted here with  $\kappa_{AB+}^{(bf)}(\lambda, T)$ ,  $\kappa_{AB+}^{(ff)}(\lambda, T)$  and  $\kappa_{AB+}^{(fb)}(\lambda, T)$ , where  $T$  is the local plasma temperature in the solar atmosphere.

However, it follows from the above mentioned that in the case  $A = \text{H}$  and  $B = \text{Si}$  we will have the transitions from two initial  $\Sigma$ - and  $\Pi$ -electronic states to two final  $\Sigma$ - and one final  $\Pi$ -electronic states. Because of that in this case we will have three groups of the spectral absorption

coefficients  $\kappa_{AB^+}^{(bf,ff,fb)}(\lambda, T; i, f)$ , which correspond to these transitions.

### 3.1 The bound-free processes.

In the usual way the spectral absorption coefficients  $\kappa_{bf}(\lambda, T)$ , which characterize the efficiency of the photo-dissociation process (3) are defined by

$$\kappa_{AB^+}^{(bf)}(\lambda, T) = \sigma_{AB^+}^{(phd)}(\lambda, T) \cdot N_{AB^+}, \quad (17)$$

where  $N(AB^+)$  is the local density of the considered molecular ion  $AB^+$ , and  $\sigma_{phd}$  is the corresponding mean thermal photo-dissociation cross section, which is given by

$$\sigma_{AB^+}^{(phd)}(\lambda, T) = \frac{\sum_{J,v} (2J+1) e^{-\frac{E_{J,v}}{kT}} \cdot \sigma_{J,v}(\lambda)}{\sum_{J,v} (2J+1) e^{-\frac{E_{J,v}}{kT}}}, \quad (18)$$

where  $\sigma_{J,v}(\lambda)$  is the partial photo-dissociation cross-section for the ro-vibrational states with given quantum numbers  $J$  and  $v$ , and  $E_{J,v}$  - the energies of these states with the respect to the ground ro-vibrational states. It means that  $E_{J,v} = E_{dis} + \epsilon_{J,v}$ , where  $E_{dis}$  is the dissociative energy of the ion  $AB^+$ , and the energies  $\epsilon_{J,v} < 0$  are determined from Eq.(7) together with the wave functions of the considered ro-vibrational states. Within the dipole approximation the partial cross-sections  $\sigma_{J,v}(\lambda)$  are given by the expressions

$$\sigma_{J,v}(\lambda) = \frac{8\pi^3}{3\lambda} \left[ \frac{J+1}{2J+1} |D_{J,v;J+1,E'_{imp}}|^2 + \frac{J}{2J+1} |D_{J,v;J-1,E'_{imp}}|^2 \right], \quad (19)$$

$$D_{J,v;J\pm 1,E'_{imp}} = \langle in, J, v; R | D_{in,fin}(R) | fin, J \pm 1, E' \rangle, \quad (20)$$

where  $E' = \epsilon_{J,v} + \epsilon_\lambda$ ,  $E'_{imp}$  and  $E'$  are connected with Eq.(11), and  $D_{in,fin}(R)$  is given by Eqs. (13) - (15).

Keeping in mind that the deviations from the local thermodynamical equilibrium (LTE) of the used model C from Vernazza et al. (1981) are not related to the considered bound-free processes, we will take the photo-dissociation coefficient  $\kappa_{AB^+}^{(bf)}(\lambda, T)$  in an equivalent form, suitable for further considerations, namely

$$\kappa_{AB^+}^{(bf)}(\lambda, T) = K_{AB^+}^{(bf)}(\lambda, T) \cdot N_A N_{B^+}, \quad (21)$$

$$K_{AB^+}^{(bf)}(\lambda, T) = \sigma_{AB^+}^{(phd)}(\lambda, T) \cdot \chi^{-1}(T; AB^+), \quad (22)$$

$$\chi(T; AB^+) = \left[ \frac{N(A)N(B^+)}{N(AB^+)} \right], \quad (23)$$

where the factor  $\chi$  is given by the relation

$$\chi(T; AB^+) = \frac{g_A g_{B^+}}{g_{AB^+}} \left( \frac{\mu kT}{2\pi \hbar^2} \right)^{\frac{3}{2}} \cdot \frac{1}{\sum_{J,v} (2J+1) e^{-\frac{E_{dis} - E_{J,v}}{kT}}}, \quad (24)$$

where  $g_{AB^+}$ ,  $g_A$  and  $g_{B^+}$  are the electronic statistical weights of the species  $AB^+$ ,  $A$  and  $B^+$  respectively, and  $\sigma_{AB^+}^{(phd)}(\lambda, T)$  is given by Eqs. (18)-(28). The behavior of the photo-dissociation cross section  $\sigma_{AB^+}^{(phd)}(\lambda, T)$  and the bound-free spectral rate coefficient  $K_{AB^+}^{(bf)}(\lambda, T)$  are illustrated in

Figs. 9 and 10, on the example of the case  $A = H$  and  $B = Mg$ , for  $110 \text{ nm} \lesssim \lambda \lesssim 205 \text{ nm}$  and  $T = 4000 \text{ K}$ ,  $T = 6000 \text{ K}$ ,  $T = 8000 \text{ K}$  and  $T = 10000 \text{ K}$ . These figures show that exist a significant difference between temperature dependence of the mean thermal photo-ionization cross section and the corresponding spectral rate coefficient.

### 3.2 The free-free processes.

The very fast approaching of the electronic dipole matrix elements  $D_{in,fin}(R)$  to zero with the increasing of  $R$  in the case of the non-symmetric ion-atom systems, which is illustrated by Figs. 6-8, makes possible to apply here the complete quantum mechanical treatment not only to the bound-free and free-bound absorption processes (3) and (5), but to the free-free absorption process (4). Namely, it can be shown (see for an example Lebedev & Presnyakov (2002)) that the free-free spectral absorption coefficients  $\kappa_{AB^+}^{(ff)}(\lambda, T)$  can be expressed over the quantities  $\sigma_{AB^+}^{(ff)}(\lambda, E) \equiv \sigma_{AB^+}^{(ff)}(J, E, \lambda; J \pm 1, E'_{imp})$  in the form

$$\begin{aligned} \kappa_{AB^+}^{(ff)}(\lambda, T) &= K_{AB^+}^{(ff)}(\lambda, T) \cdot N_A N_{B^+}, \\ K_{AB^+}^{(ff)}(\lambda, T) &= \int_0^\infty \left( \frac{2E}{\mu} \right)^{\frac{1}{2}} \sigma_{AB^+}^{(ff)}(\lambda, E) f_T(E) dE, \end{aligned} \quad (25)$$

where  $f_T(E)$  is the Maxwell impact energy distribution function

$$f_T(E) = \frac{2}{\pi^{1/2} (kT)^{3/2}} e^{-\frac{E}{k_B T}} E^{1/2} dE, \quad (26)$$

and  $\sigma_{AB^+}^{(ff)}(\lambda, E)$  is given by

$$\sigma_{AB^+}^{(ff)}(\lambda) = \frac{g_A + g_B}{g_A g_{B^+}} \frac{8\pi^4 \hbar^2 \epsilon_\lambda}{3c \cdot 2\mu E} \cdot \left[ (J+1) \cdot |D_{J,E;J+1,E'_{imp}}|^2 + J \cdot |D_{J,E;J-1,E'_{imp}}|^2 \right], \quad (27)$$

$$D_{J,E;J\pm 1,E'_{imp}} = \langle in, J, E; R | D_{in,fin}(R) | fin, J \pm 1, E' \rangle, \quad (28)$$

where  $E'_{imp}$  and  $E' = E + \epsilon_\lambda$  are connected with Eq.(11),  $g_{A^+}$ ,  $g_B$ ,  $g_A$  and  $g_{B^+}$  are the electronic statistical weights of the species  $A^+$ ,  $B$ ,  $A$  and  $B^+$  respectively. One can see that the quantity  $\sigma_{AB^+}^{(ff)}$  can be treated as the effective cross section, but is expressed in units  $\text{cm}^4$ s, and the rate coefficient  $K_{AB^+}^{(ff)}(\lambda, T)$  is equal to the absorption coefficient for the unit densities  $N(A)$  and  $N(B^+)$ .

### 3.3 The free-bound processes.

Similarly to the free-free case the free-bound spectral absorption coefficients  $\kappa_{AB^+}^{(fb)}(\lambda, T)$  is taken here as

$$\kappa_{AB^+}^{(fb)}(\lambda, T) = K_{AB^+}^{(fb)}(\lambda, T) \cdot N_A N_{B^+}, \quad (29)$$

where the rate coefficient  $K_{AB^+}^{(fb)}(\lambda, T)$  can be also expressed over the corresponding free-bound cross section. In accordance with Mihajlov & Ignjatović (1996) and Ignjatović & Mihajlov (1999) it can be presented in the form

$$K_{AB^+}^{(fb)}(\lambda, T) = \frac{(2\pi)^3}{3\hbar\lambda} \left( \frac{2\pi\hbar^2}{\mu kT} \right)^{3/2} \sum_{J',v'} \left( \frac{\mu}{2E} \right)^{1/2} e^{-\frac{E}{kT}} \cdot C_{J',v'}, \quad (30)$$

$$C_{J',v'} = \frac{g_{(AB^+)^*}}{g_A g_{B^+}} \cdot [J' | D_{J'-1, E; J', v'} |^2 + (J'+1) | D_{J'+1, E; J', v'} |^2], \quad (31)$$

$$D_{J' \pm 1, E; J', v'} = \langle in, J' \pm 1, E; R | D_{in, fin}(R) | fin, J', v' \rangle, \quad (32)$$

where  $E = I_A - I_B - \varepsilon_\lambda + \varepsilon_{J', v'}$ ,  $g_{(AB^+)^*}$  is the electronic statistical weights of the molecular ion  $(AB^+)^*$ ,  $\varepsilon_{J', v'} < 0$  -the energy of the ion  $(AB^+)^*$  in the ro-vibrational state with the orbital and vibrational quantum numbers  $J'$  and  $v'$ , and summing is performed over all these ro-vibration states. Let us note that within this paper we will neglect everywhere the corrections for stimulated emission as in all the cases considered here the corresponding corrections (given the relevant values of the ratio  $\varepsilon_\lambda/kT$ ) would be at a level of 0.01%.

The behavior of the free-free and free-bound spectral rate coefficients  $K_{AB^+}^{(ff)}(\lambda, T)$  and  $K_{AB^+}^{(fb)}(\lambda, T)$  is illustrated by the Figs. 11-13, on the examples:

$A = \text{He}$  and  $B = \text{H}$  for  $60 \text{ nm} \lesssim \lambda \lesssim 115 \text{ nm}$  and  $T = 4000 \text{ K}, 6000 \text{ K}$  and  $8000 \text{ K}$ ;

$A = \text{H}$  and  $B = \text{Mg}$  for  $150 \text{ nm} \lesssim \lambda \lesssim 220 \text{ nm}$  and  $T = 4000 \text{ K}, 6000 \text{ K}, 8000 \text{ K}$  and  $10000 \text{ K}$ ;

$A = \text{H}$  and  $B = \text{Si}$ , for the transition  $X^1\Sigma^+ \rightarrow B^1\Sigma^+$ , for  $190 \text{ nm} \lesssim \lambda \lesssim 220 \text{ nm}$  and  $T = 4000 \text{ K}, 6000 \text{ K}, 8000 \text{ K}$  and  $10000 \text{ K}$ .

These figures show that in the general case the absorption processes caused by the free-free and free-bound transitions (6) have to be considered together since their relative efficiency, characterized by  $K_{AB^+}^{(ff)}(\lambda, T)$  and  $K_{AB^+}^{(fb)}(\lambda, T)$  significantly changes from one to other ion-atom system. Let us note that at least some of the picks, existing in Figs. 11-13 which illustrate the shape of the profiles  $K_{AB^+}^{(ff)}(\lambda, T)$  and  $K_{AB^+}^{(fb)}(\lambda, T)$ , can be connected with the extremums of the corresponding splitting terms. Such phenomena in connection with the ion-atom systems were discussed already in Mihajlov & Popović (1981). Let us note that in the case of non-symmetric atom-atom systems the similar phenomena were also investigated earlier (Veža et al. 1998; Skenderović et al. 2002).

### 3.4 The partial and total non-symmetric spectral absorption coefficients.

The partial absorption coefficients which characterize the individual contribution of the considered ion-atom systems are denoted here with  $\kappa_{AB^+}(\lambda) \equiv \kappa_{AB^+}(\lambda, T; N_A, N_{B^+})$ . In accordance with the above mentioned we have that

$$\kappa_{AB^+}(\lambda) = \kappa_{AB^+}^{(bf)}(\lambda, T) + \kappa_{AB^+}^{(ff)}(\lambda, T) + \kappa_{AB^+}^{(fb)}(\lambda, T), \quad (33)$$

in the cases  $A = \text{He}$  and  $B = \text{H}$ , and  $A = \text{H}$  and  $B = \text{Mg}$  and  $\text{Al}$ ,  $\kappa_{AB^+}(\lambda)$ , and that

$$\kappa_{\text{HSi}^+}(\lambda) = \frac{1}{3}[\kappa_{\text{HSi}^+;1}(\lambda; \Sigma) + \kappa_{\text{HSi}^+;2}(\lambda; \Sigma)] + \frac{2}{3}\kappa_{\text{HSi}^+}(\lambda; \Pi), \quad (34)$$

where  $\kappa_{\text{HSi}^+;1}(\lambda; \Sigma)$  and  $\kappa_{\text{HSi}^+;2}(\lambda; \Sigma)$  describe the contribution of the radiative transitions  $X^1\Sigma^+ \rightarrow B^1\Sigma^+$  and  $X^1\Sigma^+ \rightarrow C^1\Sigma^+$  respectively, and  $\kappa_{\text{HSi}^+}(\lambda; \Pi)$  - the contribution of the transition  $A^1\Pi \rightarrow 2^1\Pi$ . The spectral absorption coefficients  $\kappa_{AB^+}^{(bf)}(\lambda, T)$ ,  $\kappa_{AB^+}^{(ff)}(\lambda, T)$  and  $\kappa_{AB^+}^{(fb)}(\lambda, T)$  are defined by Eqs. 17-24, 25-28 and 29-32 respectively.

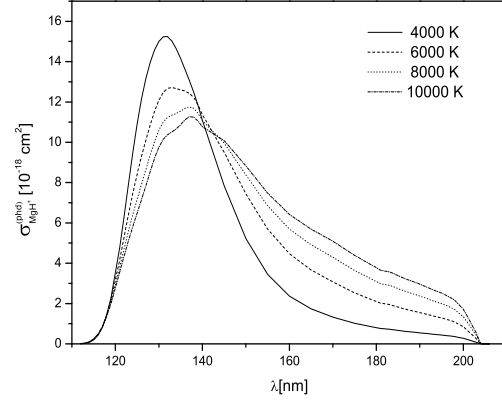


**Figure 9.** The behaviour of the mean thermal photodissociation cross-section  $\sigma_{HMg^+}^{(phd)}(\lambda; T)$  for the molecular ion  $\text{HMg}^+$ .

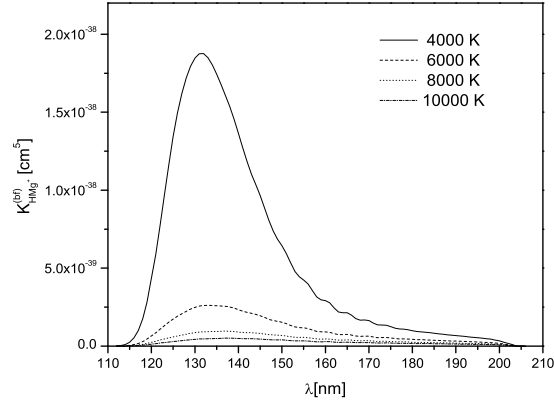


**Figure 10.** The behaviour of the bound-free (bf) spectral rate coefficient  $K_{HMg^+}^{(bf)}(\lambda; T)$  for the molecular ion  $\text{HMg}^+$ .

The total contribution of the mentioned non-symmetric ion-atom absorption processes to the opacity of the considered stellar atmospheres within this work is described by the spectral absorption coefficient  $\kappa_{ia;nsim}(\lambda) \equiv \kappa_{ia;nsim}(\lambda; T)$ , given by

$$\kappa_{ia;nsim}(\lambda) = \sum \kappa_{AB^+}(\lambda), \quad (35)$$

where the partial coefficients  $\kappa_{AB^+}(\lambda; T)$  are given by Eqs. (33) and (34), and summing is performed over all considered pairs of atom and ion species  $(A, B^+)$ . It is assumed that these coefficients are determined with the plasma temperature  $T$  and the atom and ion densities taken from the used model of the considered atmosphere.

## 4 RESULTS AND DISCUSSION

The absorption coefficients, as functions of the plasma's temperature and the atomic and ionic densities in the solar pho-

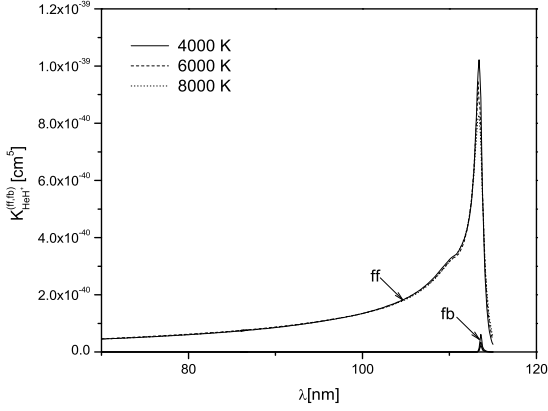


**Figure 11.** The behavior of the free-free (ff) and free-bound (fb) spectral rate coefficients  $K^{(ff,fb)}(\lambda; T)$  for  $\text{HeH}^+$ .

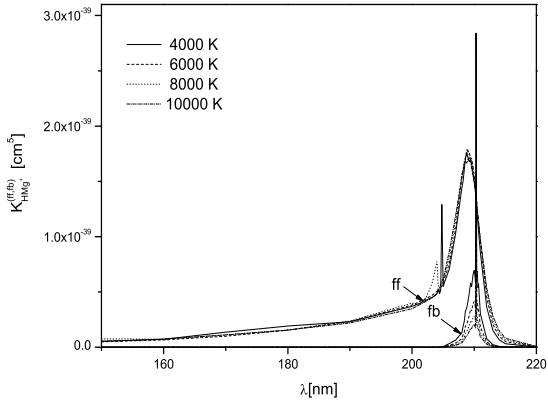


**Figure 12.** Same as in Fig.11, but for  $\text{HMg}^+$ .

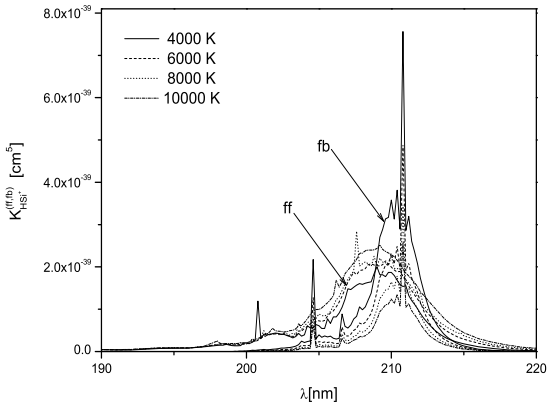


**Figure 13.** Same as in Fig.11, but for the transition  $X^1\Sigma^+ \rightarrow B^1\Sigma^+$  for  $\text{HSi}^+$ .

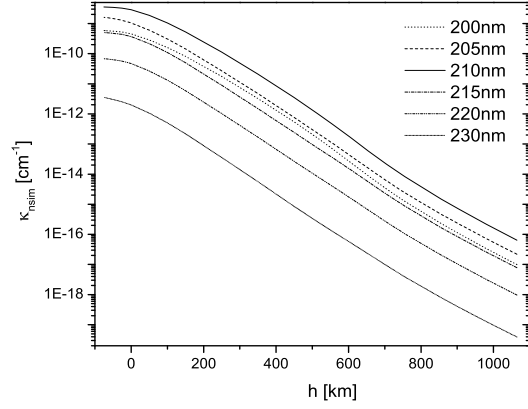


**Figure 14.** Quiet Sun. Spectral absorption coefficient  $\kappa_{nsim}(\lambda, T)$ , given by equation (36) for  $200 \text{ nm} \leq \lambda \leq 230 \text{ nm}$ .

tosphere, are determined here based on the non-equilibrium model C from Vernazza et al. (1981), where these parameters are presented as functions of the height ( $h$ ) of the considered layer with respect to the chosen referent layer. The total non-symmetric spectral absorption coefficient  $\kappa_{ia;nsim}(\lambda)$  is taken here, in accordance with Eq. (35), in the form

$$\kappa_{ia;nsim}(\lambda) = \kappa_{\text{HeH}^+}(\lambda) + \kappa_{\text{HMg}^+}(\lambda) + \kappa_{\text{HSi}^+}(\lambda), \quad (36)$$

where the partial spectral absorption coefficients  $\kappa_{AB^+}(\lambda)$  are determined using the above expressions for the  $bf$ ,  $ff$  and  $fb$  rate coefficients. The results of the calculations of  $\kappa_{ia;nsim}(\lambda)$  as a function of  $h$ , for  $-75 \text{ km} \leq h \leq 1100 \text{ km}$  are presented in Figs. 14-16 which cover the part of UV and EUV region where  $40 \text{ nm} \leq \lambda \leq 230 \text{ nm}$ . Consequently, this part covers all regions of  $\lambda$  relevant for the considered ion-atom systems (see Figs. 9-13). In accordance with this, Fig. 14 illustrates the common contribution of the  $\text{HMg}^+$  and  $\text{HSi}^+$  absorption continua, while Fig. 15 refers to the region of exclusive domination of the  $\text{HMg}^+$  continuum. Finally, the Fig. 16 illustrates the  $\text{HeH}^+$  absorption continuum.

As the characteristics of the non-symmetric absorption processes (3)-(5), in the context of their influence on the solar atmosphere opacity, here it is used the quantity  $G_{tot}^{(nsim)}(\lambda)$  defined by the relations

$$G_{tot}^{(nsim)}(\lambda) = \frac{\kappa_{ia;nsim}(\lambda)}{\kappa_{ia;tot}(\lambda)}, \quad \kappa_{ia;tot}(\lambda) = \kappa_{ia;nsim}(\lambda) + \kappa_{ia;sim}(\lambda), \quad (37)$$

where  $\kappa_{ia;sim}(\lambda)$  characterize the contribution of the symmetric ion-atom absorption processes (1) and (2). In accordance with these relations the quantity  $G_{tot}^{(nsim)}(\lambda)$  describes the relative contribution of the non-symmetric processes (3)-(5) to the total absorption caused by all ion-atom absorption processes. Let us note that the use of  $\kappa_{ia;sim}(\lambda)$  as a referent quantity is justified as these symmetric processes are now already included in some solar atmosphere models (Fontenla et al. 2009).

It is clear that apart of the quantity  $G_{tot}^{(nsim)}(\lambda)$  as the characteristics of the processes (3)-(5) could be used some other quantities, e.g. the ratio  $\kappa_{ia;tot}(\lambda)/\kappa_{ia;sim}(\lambda)$ , which describes the direct increase of the efficiency of the



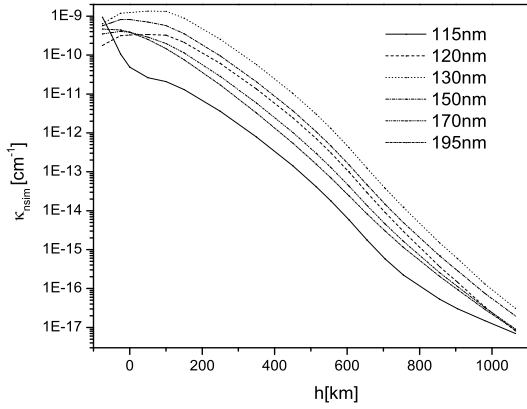


Figure 15. Same as in Fig.14, but for  $115 \text{ nm} \leq \lambda \leq 195 \text{ nm}$ .

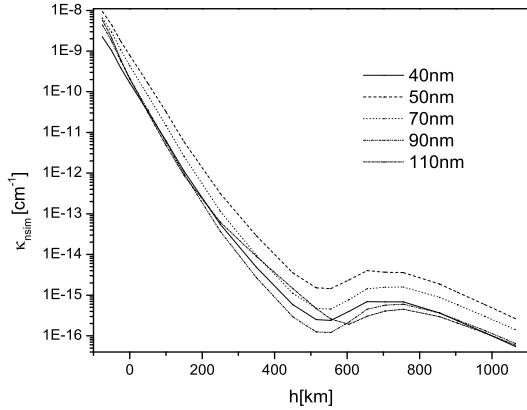


Figure 16. Same as in Fig.14, but for  $40 \text{ nm} \leq \lambda \leq 110 \text{ nm}$ .

ion-atom absorption processes caused by the inclusion of the non-symmetric ones. However, in the case of the solar atmosphere it would be very difficult to use this ratio. Namely, in accordance with Vernazza et al. (1981) in the part of the solar atmosphere around its temperature minimum the proton densities  $N_{H^+} \ll N_{B^+}$ , where  $B = \text{Mg}$  and  $\text{Si}$ , and consequently the quantity  $[\kappa_{ia;nsim}(\lambda) + \kappa_{ia;sim}(\lambda)]/\kappa_{ia;nsim}(\lambda) \gg 1$ . Consequently, the behavior of this quantity can be hardly shown in the whole region of  $h$  in the same proportion. Because of that, as the characteristic of the significance of the non-symmetric absorption processes (3)-(5) for the solar atmosphere in UV and EUV region, the quantity  $G_{tot}^{(nsim)}(\lambda)$  is used, since from its definition follows that always  $0 < G_{tot}^{(nsim)}(\lambda) < 1$ . The values of  $\kappa_{ia;sim}(\lambda)$ , needed for the  $G_{tot}^{(nsim)}(\lambda)$  determination, are taken from Mihajlov et al. (2007).

The calculated values of  $G_{tot}^{(nsim)}(\lambda)$  as function of  $h$ , for the chosen set of  $\lambda$ , are presented in Figs.17-19. From these figures one can see that around the mentioned temperature minimum ( $T \lesssim 5000 \text{ K}$ ,  $150 \text{ km} \lesssim h \lesssim 705 \text{ km}$ ) the contribution of non-symmetric processes (3)-(5) are dominant in

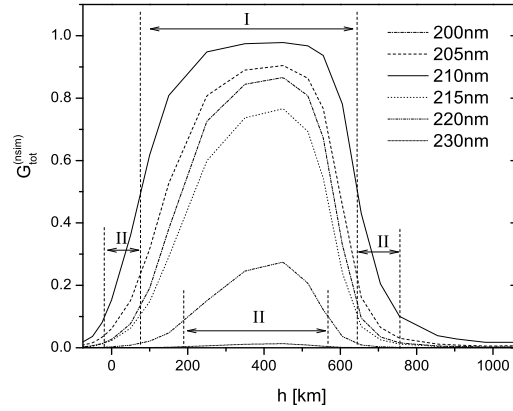


Figure 17. The presented values of  $G_{tot}^{(nsim)}(\lambda)$ , given by equation (37), as the function of  $h$  for the quiet Sun for  $200 \text{ nm} \leq \lambda \leq 230 \text{ nm}$ ; I and II are the regions of  $h$  where  $0.5 \lesssim G_{tot}^{(nsim)}(\lambda)$  and  $0.1 \lesssim G_{tot}^{(nsim)}(\lambda) < 0.5$  respectively.

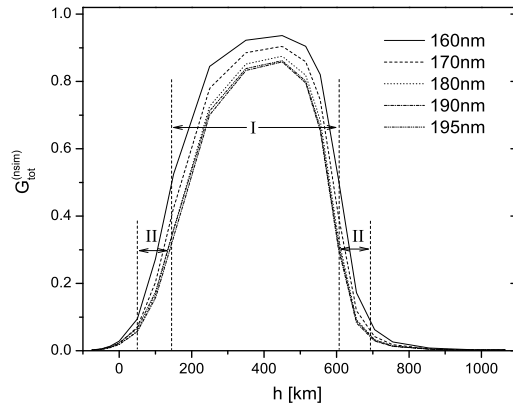


Figure 18. Same as in Fig.17, but for  $160 \text{ nm} \leq \lambda \leq 195 \text{ nm}$ .

respect to the symmetric processes (1) and (2). Such region of the non-symmetric processes domination is denoted in these figures as the region "I". Apart of that, Figs. 17-19 show that within the rest of the considered region of  $h$  there are significant parts where the relative contribution of the non-symmetric processes is close to or at least comparable with the contribution of the symmetric ones. In the same figures these parts are denoted as regions "II".

In order to additionally show the importance of the considerations in the case of the solar atmosphere of the non-symmetric processes (3)-(5) here, similarly to Mihajlov et al. (2007), it was performed the comparison of the efficiencies of the ion-atom absorption processes and the efficiency of such concurrent processes as the ion  $\text{H}^-$  photo-detachment and the electron-hydrogen atom inverse "bremsstrahlung" ( $\text{H}^-$  continuum). Namely, among relevant concurrent absorption processes just these electron-atom ones can be treated until now as the dominant in the spec-

tral region which was considered in Mihajlov et al. (2007). For that purpose in this work it was compared the behavior of the quantity

$$F_{ea}^{(sim)}(\lambda) = \frac{\kappa_{ia;sim}(\lambda)}{\kappa_{ea}(\lambda)}, \quad (38)$$

which is similar to the correspond quantity from Mihajlov et al. (2007) and characterize the relative efficiency of the ion-atom symmetric processes and  $H^-$  continuum, and the quantity

$$F_{ea}^{(tot)}(\lambda) = \frac{\kappa_{ia;tot}(\lambda)}{\kappa_{ea}(\lambda)}, \quad (39)$$

which characterize the increasing of the total efficiency of the ion-atom radiative processes after the including in the consideration of the non-symmetric processes (3)-(5). In these expressions  $\kappa_{ia;tot}(\lambda)$  is given by Eq.(37), the spectral absorption coefficient  $\kappa_{ia;sim}(\lambda)$  characterizes the ion-atom symmetric processes (1) and (2) and is taken from Mihajlov et al. (2007), and the spectral absorption coefficient  $\kappa_{ea}(\lambda)$  describes the  $H^-$  continuum. In the case of the solar atmosphere  $\kappa_{ea}(\lambda)$  is determined based on of Stillely & Callaway (1970), Wishart (1979) and Vernazza et al. (1981). The behavior of  $F_{ea}^{(sim)}(\lambda)$  and  $F_{ea}^{(tot)}(\lambda)$ , as the functions of  $h$ , is presented in Fig.20. This figure shows that the inclusion in the consideration of the non-symmetric processes (3)-(5) causes the significant increases of the total efficiency of the ion-atom absorption processes, particularly in the neighborhood of the solar atmosphere temperature minimum, where it become close to the efficiency of the  $H^-$  continuum.

In connection with the above mentioned let us note that according to Vernazza et al. (1981) in the neighborhood of the solar atmosphere temperature minimum ( $50 \text{ km} \lesssim h \lesssim 650 \text{ km}$ ) the Fe component gives the maximal individual contribution to the electron density in respect to the Mg and Si components. It means that the inclusion in the consideration of the processes (3)-(5) with  $A = H$  and  $B = Fe$  would surely significantly increase the total contribution of the non-symmetric ion-atom absorption processes, perhaps for about 50%. Because of that we have as the task for the nearest future to find the data about the relevant characteristics of the molecular ion  $HFe^+$ , since the data from Vernazza et al. (1981) make possible to perform all needed calculations.

Let us note also that, according to the data from Vernazza et al. (1981) and Fontenla et al. (2009), in the solar atmosphere it should be include in the consideration the non-symmetric processes (3)-(5) with  $A = H$ , where  $B$  is the atom of the one of such components (C, Al etc.), which give visible contribution in narrow regions of  $h$  and  $\lambda$ . Now we have only the data needed for the case  $A = H$  and  $B = Al$ , whose contribution is noticeable in the region  $140 \text{ nm} \lesssim \lambda \lesssim 155 \text{ nm}$ . Since there is a certain difference between shapes of the lower potential curves for the ion  $AlH^+$ , presented in Fig. 5 and the corresponding figure from Guest & Hirst (1981), whose nature by now is not completely clear, the contribution of the processes (3)-(5) with  $A = H$  and  $B = Al$  was not included in the calculations described above. However, we think that this contribution can serve to estimate the usefulness of the inclusion in the consideration of these processes. For that purpose we pre-

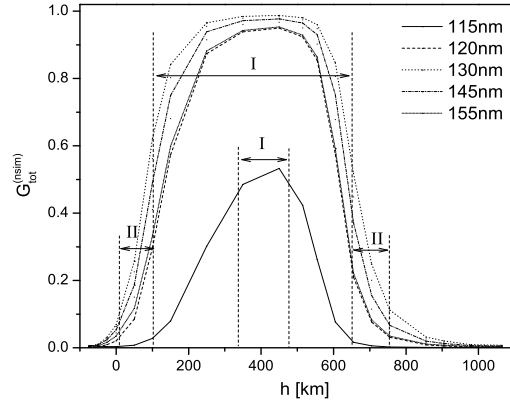


**Figure 19.** Same as in Fig.17, but for  $115 \text{ nm} \leq \lambda \leq 155 \text{ nm}$ .

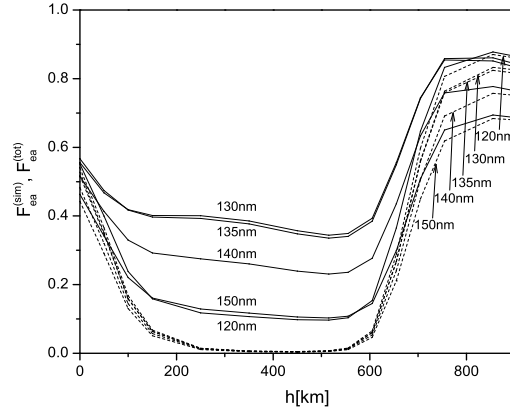


**Figure 20.** Quantities  $F_{ea}^{(sim)}(\lambda)$  (dashed line) and  $F_{ea}^{(tot)}(\lambda)$  (full line), defined in equations (38) and (39) as the functions of  $h$  for the Solar atmosphere for  $120 \text{ nm} \leq \lambda \leq 150 \text{ nm}$ .

sented in Fig. 21 the results of the calculations of the ratios  $(\kappa_{ia;nsim}(\lambda) + \kappa_{AlH^+}(\lambda))/\kappa_{ia;nsim}(\lambda)$ , as function of  $h$ , for  $140 \text{ nm} \leq \lambda \leq 155 \text{ nm}$ , where  $\kappa_{ia;nsim}(\lambda)$  was determined according to Eq.36. The behavior of this ratios presented in above mentioned figure, in the region  $200 \text{ km} < h < 700 \text{ km}$ , is caused by the fast decreases of the corresponding ion species concentration. This figure clearly demonstrate the fact that in the significant parts of the solar photosphere the inclusion in the consideration of the processes (3)-(5) with  $A = H$  and  $B = Al$  should noticeably increase the total contribution of the non-symmetric ion-atom processes. The above mentioned suggest that the contribution of all metal components which by now were not included in the consideration could significant increase the total efficiency of the ion-atom radiative processes, which is characterized by the quantity  $F_{ea}^{(tot)}(\lambda)$  in Fig.20. The results presented in Figs.17-19 and 20 shows that the neglecting of the contribution of the non-symmetric processes (3)-(5) to the opacity of the solar atmosphere, in respect to the contribution of symmetric processes

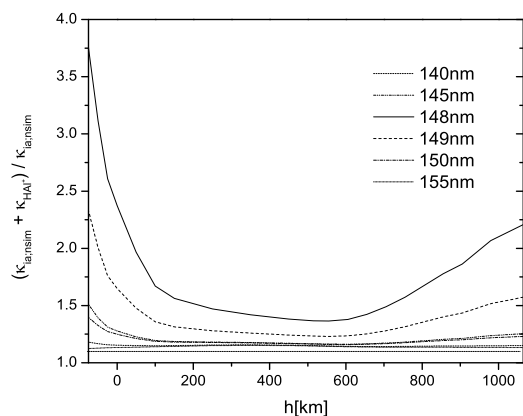


**Figure 21.** The ratio  $(\kappa_{ia;nsim}(\lambda) + \kappa_{AIH^+}(\lambda)) / \kappa_{ia;nsim}(\lambda)$ , where  $\kappa_{ia;nsim}(\lambda)$  is given by equation (36) and  $\kappa_{AIH^+}(\lambda)$  by equation (33) for  $A = H$  and  $B = Al$ , as a function of  $h$  for the Solar atmosphere for  $140 \text{ nm} \leq \lambda \leq 155 \text{ nm}$ .

(1) and (2) would caused significant errors. From here it follows that the non-symmetric absorption processes (3)-(5) should be *ab initio* included in the solar atmosphere models.

## 5 CONCLUSIONS

From the presented material it follows that the considered non-symmetric ion-atom absorption processes can not be treated only as one channel among many equal channels with influence on the opacity of the solar atmosphere. Namely, these non-symmetric processes around the temperature minimum increase the absorption of the EM radiation, which is caused by all (symmetric and non-symmetric) ion-atom absorption processes, so that this absorption becomes almost uniform in the whole solar photosphere. Moreover, the presented results show that further investigations of these processes promise to demonstrate that they are of similar importance as the known process of photo-detachment of the ion  $H^-$ , which was treated until recently as absolutely dominant. Namely, the inclusion of the non-symmetric absorption processes into consideration with  $A = H$  and  $B = Fe$ , as well as some other similar processes (with  $A = H$  and  $B = Al$  etc), would significantly increase the contribution of such processes to the solar-atmosphere opacity. All mentioned facts suggest that the considered non-symmetric ion-atom absorption processes should be included *ab initio* in the solar-atmosphere models, as well as in the models of solar and near solar type stars.

## ACKNOWLEDGMENTS

The authors wish to thank to Profs. V.N. Obridko and A.A. Nusinov for the shown attention to this work. Also, the authors are thankful to the Ministry of Education, Science and Technological Development of the Republic of Serbia for the support of this work within the projects 176002, III4402.

## REFERENCES

- Dunning, Jr., T. H. 1989, J. Chem. Phys., 90, 1007  
 Fontenla, J. M., Curdt, W., Haberleiter, M., Harder, J., & Tian, H. 2009, ApJ, 707, 482  
 Green, T. A., Browne, J. C., Michels, H. H., & Madsen, M. M. 1974a, J. Chem. Phys., 61, 5198  
 Green, T. A., Michels, H. H., Browne, J. C., & Madsen, M. M. 1974b, J. Chem. Phys., 61, 5186  
 Guest, M. F., & Hirst, D. M. 1981, Chem. Phys. Lett., 84, 167  
 Ignjatović, L. M., & Mihajlov, A. A. 1999, in Vedel F., ed., Proceedings of the 31st EGASConference of the European Group for Atomic Spectroscopy. Royal Swedish Academy of Sciences, Stockholm, p. P2  
 Kendall, R. A., Dunning, Jr., T. H., & Harrison, R. J. 1992, J. Chem. Phys., 96, 6796  
 Lebedev, V. S., & Presnyakov, L. P. 2002, J. Phys. B: At. Mol. Opt. Phys., 35, 4347  
 Mihajlov, A. A., & Dimitrijević, M. S. 1986, A&A, 155, 319  
 Mihajlov, A. A., & Ignjatović, L. M. 1996, Dynamique des Ions, des Atomes et desMolecules (DIAM 96) Bourges, France 15-18 Jul 1996, Contrib. Papers, p. 157  
 Mihajlov, A. A., & Popović, M. P. 1981, Phys. Rev. A, 23, 1679  
 Mihajlov, A. A., Dimitrijević, M. S., & Ignjatović, L. M. 1993, A&A, 276, 187  
 Mihajlov, A. A., Dimitrijević, M. S., Ignjatović, L. M., & Djurić, Z. 1994b, A&AS, 103, 57  
 Mihajlov, A. A., Ignjatović, L. M., Sakan, N. M., & Dimitrijević, M. S. 2007, A&A, 437, 1023  
 MOLPRO. 2006, in MOLPRO is a package of programs written by H.J. Werner and P.J. Knowles with contributions from J. Almlof et al, <http://www.molpro.net>  
 Skenderović, H., Beuc, R., Ban, T., & Pichler, G. 2002, European Physical Journal D, 19, 49  
 Stille, J. L., & Callaway, J. 1970, ApJ, 160, 245  
 Stix, M. 2002, The sun: An Introduction, Springer, Heidelberg  
 Vernazza, J., Avrett, E., & Loser, R. 1981, ApJS, 45, 635  
 Veža, D., Beuc, R., Milošević, S., & Pichler, G. 1998, European Physical Journal D, 2, 45  
 White, O. R. 1977, The Solar Output and its Variation. Proceedings of a Workshop, Colorado, April, 1976. Edited by Oran R. White. Boulder: Colorado Associated University Press, 1977  
 Wishart, A. W. 1979, MNRAS, 187, 59  
 Woods, T. 2008, Advances in Space Research, 42, 895  
 Woods, T., Chamberlin, P., Harder, J., Hock, R., Snow, M., Eparvier, F., Fontenla, J., McClintock, W. & Richard, E. 2009, Geophysical research letters, 36, L01101  
 Worden, J., Woods, T., & Bowman, K. 2001, ApJ, 560, 1020